Bucknell University
Bucknell Digital Commons

Faculty Journal Articles | Faculty Scholarship

2015

Restricted Salt Diffusion in a Geosynthetic Clay Liner

Michael A. Malusis
Bucknell University, mam028@bucknell.edu

Jong Beom Kang

Charles D. Shackelford
Colorado State University - Fort Collins

Follow this and additional works at: https://digitalcommons.bucknell.edu/fac_journ

Part of the Environmental Engineering Commons, and the Geotechnical Engineering Commons

Recommended Citation

Malusis, Michael A.; Kang, Jong Beom; and Shackelford, Charles D.. "Restricted Salt Diffusion in a Geosynthetic Clay Liner." *Environmental Geotechnics* (2015) : 68-77.

This Article is brought to you for free and open access by the Faculty Scholarship at Bucknell Digital Commons. It has been accepted for inclusion in Faculty Journal Articles by an authorized administrator of Bucknell Digital Commons. For more information, please contact dcadmin@bucknell.edu.

Environmental Geotechnics

Restricted salt diffusion in a geosynthetic clay liner
Malusis, Kang and Shackelford

Environmental Geotechnics
http://dx.doi.org/10.1680/envgeo.13.00080
Paper 13.00080
Received 02/08/2013; accepted 05/11/2013
Keywords: environment/geotechnical engineering/waste management & disposal

ICE Publishing: All rights reserved

ice
Institution of Civil Engineers
publishing

Restricted salt diffusion in a geosynthetic clay liner

1 **Michael A. Malusis** PhD, PE
Associate Professor, Department of Civil and Environmental Engineering, Bucknell University, Lewisburg, PA, USA

2 **Jong-Beom Kang** PhD, PE
Geotechnical Engineer, Engineering Analytics, Inc., Fort Collins, CO, USA

3 **Charles D. Shackelford** PhD, PE
Professor, Department of Civil and Environmental Engineering, Colorado State University, Fort Collins, CO, USA

The influence of semipermeable membrane behaviour on salt diffusion through a geosynthetic clay liner (GCL) was investigated by conducting multi-stage membrane tests on four GCL specimens at different effective stresses (σ' = 34·5–242 kPa) in flexible-wall cells. Each test was conducted by circulating five source potassium chloride solutions, sequentially from lowest to highest concentration (C_o = 3·9, 6·0, 8·7, 20, 47 mM), across the top specimen boundary, while circulating de-ionized water across the bottom boundary. Membrane efficiency coefficients (ω) were determined from differential pressure measurements, and effective salt-diffusion coefficients (D_s^*) were inferred from boundary electrical conductivities. Increases in D_s^* with increasing C_o were observed for all specimens and were correlated to decreases in ω. In each case, D_s^* decreased linearly toward zero as $\omega \rightarrow 1$, regardless of the applied σ'. These results support the hypothesis from pore-scale physical modelling that D_s^* for GCLs exhibiting membrane behaviour may be expressed as a linear function of the quantity $1 - \omega$.

Notation

C	molar solute concentration
D_s^*	effective salt-diffusion coefficient
D_{so}	free-solution salt-diffusion coefficient
D_{se}	matrix salt-diffusion coefficient
EC	electrical conductivity
J^d	diffusive solute flux
L	GCL specimen thickness
P	pressure
Q_t	cumulative moles of diffused solute
R	universal gas constant
T	absolute temperature
n	total porosity
n_e	effective porosity
t	time
x	direction of transport
θ	ratio of effective to total porosity
σ'	effective stress
τ_a	apparent tortuosity factor
τ_m	matrix tortuosity factor
τ_r	restrictive tortuosity factor
ω	membrane efficiency coefficient

Introduction

The ability of clays to act as semipermeable membranes that inhibit the passage of solutes while allowing relatively unimpeded migration of water is well recognized. Although much of the historical literature on membrane behaviour pertains to natural clays and shales (e.g., Greenberg *et al.*, 1973; Kharaka and Berry, 1973; Marine and Fritz, 1981; Neuzil, 1986; Young and Low, 1965), many of the more recent studies have investigated such behaviour in engineered clay barriers used for geoenvironmental containment, including geosynthetic clay liners (GCLs), compacted clay liners, and soil-bentonite vertical cutoff walls (e.g., Henning *et al.*, 2006; Kang and Shackelford, 2010, 2011; Keijzer *et al.*, 1999; Malusis and Shackelford, 2002a,b; Mazzieri *et al.*, 2010; Shackelford, 2013; Yeo *et al.*, 2005). These studies show that GCLs are most likely to exhibit significant membrane behaviour owing to the high content of sodium bentonite in these barriers. Such behaviour can improve the containment performance of a GCL by reducing the flux of aqueous miscible contaminants through the GCL due to hyperfiltration, chemico-osmotic flow, and restricted diffusion (Malusis *et al.*, 2003).

Regarding restricted diffusion, experimental studies have shown that the effective salt-diffusion coefficient, D_s^*, for GCL-type

specimens tends to decrease with an increase in the membrane efficiency coefficient, ω (Di Emidio, 2010; Dominijanni, 2013; Malusis and Shackelford, 2002b). This effect of decreasing D_s^* with increasing ω has been referred to as "implicit coupling," because the effect is not explicitly captured in macro-scale theoretical formulations for coupled solute flux based on nonequilibrium thermodynamics (e.g., Malusis and Shackelford, 2002b, 2004a,b; Malusis *et al.*, 2012). Theoretical studies by Dominijanni (2005) and Dominijanni and Manassero (2012) based on physical modelling at the pore scale have shown that D_s^* may be approximated as a linear function of the quantity $1 - \omega$. However, the validity of this linear function for GCLs is supported by limited experimental data (Dominijanni *et al.*, 2013; Malusis *et al.*, 2012) and has not yet been investigated for GCL specimens tested under different stress conditions.

In this study, the influence of ω on D_s^* for GCLs was investigated using the results of multi-stage membrane tests conducted by Kang (2008) on GCL specimens, each consolidated under a different effective stress (σ'). The ω values for these specimens were reported previously by Kang and Shackelford (2011). The diffusion results presented herein were inferred from the tests of Kang (2008) and are used to further assess the validity of the linear relationship between D_s^* and $1 - \omega$.

Background

Consider a salt-diffusion experiment in which a clay membrane is placed in a closed system between two sealed reservoirs, as illustrated in Figure 1. The source reservoir contains a binary salt (potassium chloride) solution, whereas the collection reservoir contains de-ionized water (DIW). The diffusive molar fluxes, J^d, of the salt cation (c) and the salt anion (a) may be expressed as follows based on Fick's law:

1. $$J_c^d = -nD_s^* \frac{\partial C_c}{\partial x}; \quad J_a^d = -nD_s^* \frac{\partial C_a}{\partial x}$$

where n is total porosity and C_c and C_a are the molar concentrations of the cation and anion, respectively. The effective salt-diffusion coefficient, D_s^*, is defined as the product of the salt-diffusion coefficient in free solution, D_{so}, and the apparent tortuosity factor,

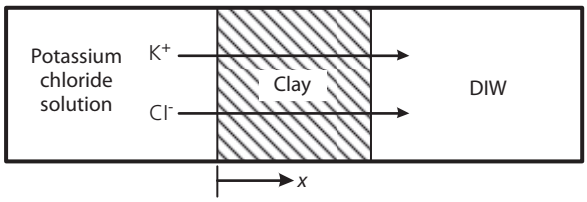

Figure 1. Salt diffusion of potassium chloride through a clay in a closed system (DIW, de-ionized water)

τ_a (i.e., $D_s^* = \tau_a D_{so}$), whereas τ_a can be expressed as the product of a matrix tortuosity factor, τ_m, and a restrictive tortuosity factor, τ_r, as follows (Malusis and Shackelford, 2002b):

2. $$\tau_a = \tau_m \tau_r = \tau_m \prod_{i=1}^{N} \tau_i$$

where τ_m accounts for tortuosity associated with the geometry of the interconnected pores and τ_r accounts for any number (N) of other mechanisms (represented by τ_i) that restrict diffusion, such as solute exclusion and solute drag near particle surfaces (e.g., Kemper *et al.*, 1964; Shackelford and Daniel, 1991; Shackelford and Moore, 2013). Based on Equation 2, D_s^* may be written as follows:

3. $$D_s^* = \tau_r \tau_m D_{so} = \tau_r D_{se}$$

where D_{se} ($= \tau_m D_{so}$) is termed herein the matrix salt-diffusion coefficient or the effective salt-diffusion coefficient that accounts only for the matrix tortuosity.

Since τ_m is associated solely with the geometric interconnectivity of the pores, τ_m and D_{se} generally are considered constant for a given arrangement of soil particles and, therefore, independent of solute concentration. In contrast, τ_r for clay membranes decreases with increasing ω (Malusis and Shackelford, 2002b). Theoretically, $\tau_r = 0$ for ideal membranes ($\omega = 1$) that completely exclude solute migration. However, higher solute concentrations cause shrinkage of the diffuse double layers (DDLs) surrounding the clay particles and a decrease in ω, such that $\tau_r \to 1$ as $\omega \to 0$, assuming that all other potentially restrictive effects are insignificant. Under this assumption, D_s^* ($\omega = 0$) = D_{se} based on Equation 3.

Alternatively, restricted diffusion in clay membranes may be represented as a porosity restriction, where the effective porosity, n_e, available for solute migration is less than n (e.g., see Shackelford and Moore, 2013). On this basis, Manassero and Dominijanni (2003) expressed τ_r in Equation 3 as an effective porosity ratio, θ ($= n_e/n$, where $n_e = n$ and $\theta = 1$ when $\omega = 0$, and $n_e = \theta = 0$ when $\omega = 1$). Furthermore, Manassero and Dominijanni (2003) proposed that θ ($= \tau_r$) may be approximated as a simple, linear function of ω, as follows:

4. $$\theta = \tau_r = 1 - \omega$$

Substitution of Equations 3 and 4 into Equation 1 yields the following alternative expressions for diffusive flux of the cation and anion in Figure 1:

5. $$J_c^d = -n(1-\omega)D_{se} \frac{\partial C_c}{\partial x}; \quad J_a^d = -n(1-\omega)D_{se} \frac{\partial C_a}{\partial x}$$

Although Equation 4 is supported theoretically on the basis of physical modelling at the pore scale, that is, provided that pore-scale variations in pressure, ion concentration, and water velocity within the membrane are negligible (Dominijanni, 2005; Dominijanni and Manassero, 2012; Dominijanni *et al.*, 2013), experimental support for the validity of Equation 4 is limited. For example, measured values of D_s^* reported in the literature for GCL or GCL-type specimens subjected to inorganic salt (potassium chloride, sodium chloride, or calcium chloride) solutions (Di Emidio, 2010; Dominijanni *et al.*, 2013; Malusis and Shackelford, 2002b) are plotted as a function of ω in Figure 2a. The corresponding values of τ_r computed using Equation 3 (where D_{se} is determined by extrapolation of D_s^* to the $\omega = 0$ axis in Figure 2a) generally follow the linear trend defined by Equation 4, as illustrated in Figure 2b. However, given the paucity of data and the scatter in Figure 2b ($R^2 = 0{\cdot}64$), additional data are needed to bolster the validity of Equation 4.

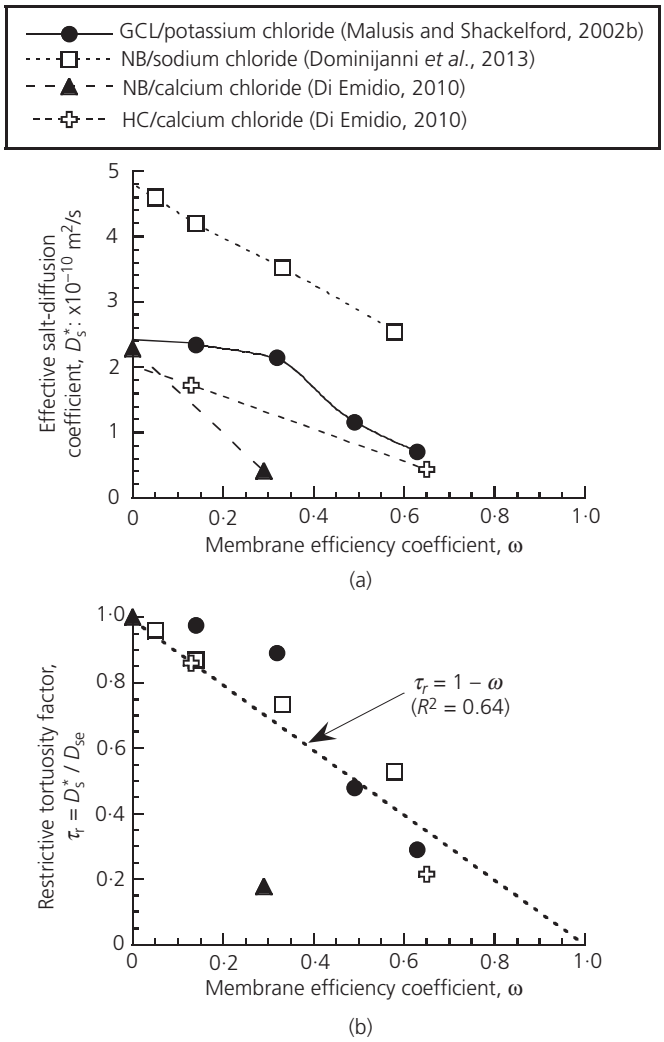

Figure 2. Effective salt-diffusion coefficients (a) and restrictive tortuosity factors (b) for bentonite specimens in potassium chloride, sodium chloride, or calcium chloride solutions (GCL, geosynthetic clay liner; NB, sodium bentonite; HC, HYPER clay)

Materials and methods

GCL and potassium chloride solutions

The GCL in this study is the same as that used by Malusis and Shackelford (2002b) and is sold as Bentomat® by Colloid Environmental Technologies Co. (CETCO, USA). As described by Kang and Shackelford (2011), the bentonite component of the GCL contained 71% montmorillonite and 53% sodium on the exchange sites. The measured cation exchange capacity was 47·7 cmol$_c$/kg, and the liquid limit and plasticity index were 478 and 439, respectively.

The potassium chloride solutions used in this study ranged in concentration from 3·9 to 47 mM and were prepared by dissolving potassium chloride crystals in DIW. The relationship between electrical conductivity, EC, and salt concentration for these solutions is illustrated in Figure 3, along with the same relationship for similarly prepared sodium chloride solutions, for comparison. The fitted equation for EC as a function of potassium chloride concentration was used to estimate boundary potassium chloride concentrations during the membrane tests, as discussed further in below.

Testing apparatus

The testing apparatus, illustrated in Figure 4, consisted of a flexible-wall cell and a hydraulic control system (syringe pump and stainless steel tubing) to circulate different solutions across the boundaries of the GCL specimen. During membrane testing, the source potassium chloride solution ($C_{ot} > 0$) and DIW ($C_{ob} = 0$) were circulated across the top and bottom of the specimen, respectively, under closed-system conditions such that volume change within the

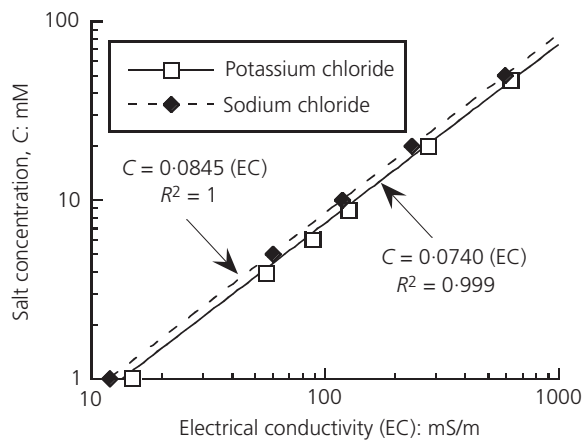

Figure 3. Relationship between measured electrical conductivity and salt concentration for potassium chloride and sodium chloride solutions at 25°C

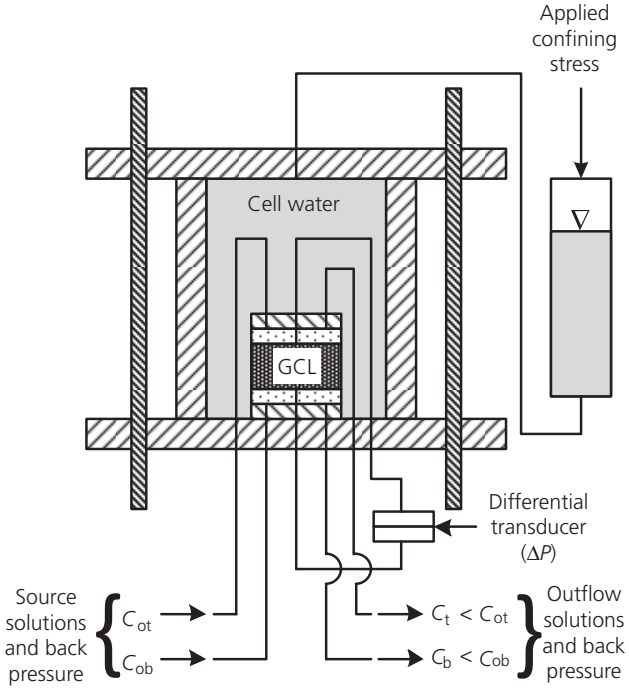

Figure 4. Schematic of flexible-wall membrane/diffusion test apparatus (adapted from Kang and Shackelford, 2011)

system was prevented. The applied difference in potassium chloride concentration across the specimen induced a pressure difference (owing to the prevention of chemico-osmotic liquid flux through the specimen) that was measured with a differential pressure transducer. Furthermore, salt diffusion through the specimen resulted in collection of solutes in the DIW circulating across the bottom boundary, such that the solute concentration exiting the bottom boundary, C_b, was greater than that in the DIW (i.e., $C_b > C_{ob}$). This difference between C_b and C_{ob} provided the basis for determining D_s^* for the specimen. Further details of the apparatus are provided by Kang and Shackelford (2009, 2010, 2011).

Specimen preparation

Four circular specimens of the GCL, with nominal diameters of 102 mm and thicknesses of 10 mm, were cut from a larger GCL sheet and placed on the base pedestal of a flexible-wall permeameter. Each specimen was subjected to an effective stress, σ', of 34·5 kPa (5 psi) under 172 kPa (25 psi) of back pressure and permeated with DIW to saturate the specimen, measure the baseline hydraulic conductivity, k, and remove most of the soluble salts initially contained within the specimen. After permeation, the specimens were transferred to the flexible-wall membrane cells (Figure 4) and again subjected to σ' = 34·5 kPa. Once consolidation reached completion under σ' = 34·5 kPa, three of the four specimens were further consolidated under final values of σ' = 103 kPa (15 psi), 172 kPa (25 psi) or 241 kPa (35 psi) by increasing the cell pressure in a single loading step (the back pressure of 172 kPa (25 psi) was maintained constant in all tests). Changes in specimen height were estimated based on changes in porosity computed using measured changes in cell-water volume. The drainage (back-pressure) lines were closed after the consolidation stage and before the start of the membrane/diffusion tests (for more details, see Kang and Shackelford, 2011).

Membrane testing

The membrane tests were initiated by circulating DIW through the top and bottom boundaries of each specimen at a circulation rate of $4{\cdot}2 \times 10^{-10}$ m³/s for 7 days to establish a steady baseline pressure difference. This circulation rate has been proven to be sufficiently fast to maintain reasonably constant concentration boundaries (Malusis *et al.*, 2001). The membrane efficiency measurements were then initiated by circulating the 3·9-mM potassium chloride solution across the top specimen boundary while continuing the circulation of DIW across the bottom boundary. The differential pressure induced across each specimen, ΔP, and the EC of the solutions exiting the top and bottom boundaries (EC_t and EC_b, respectively) were measured until ΔP, EC_t, and EC_b became steady.

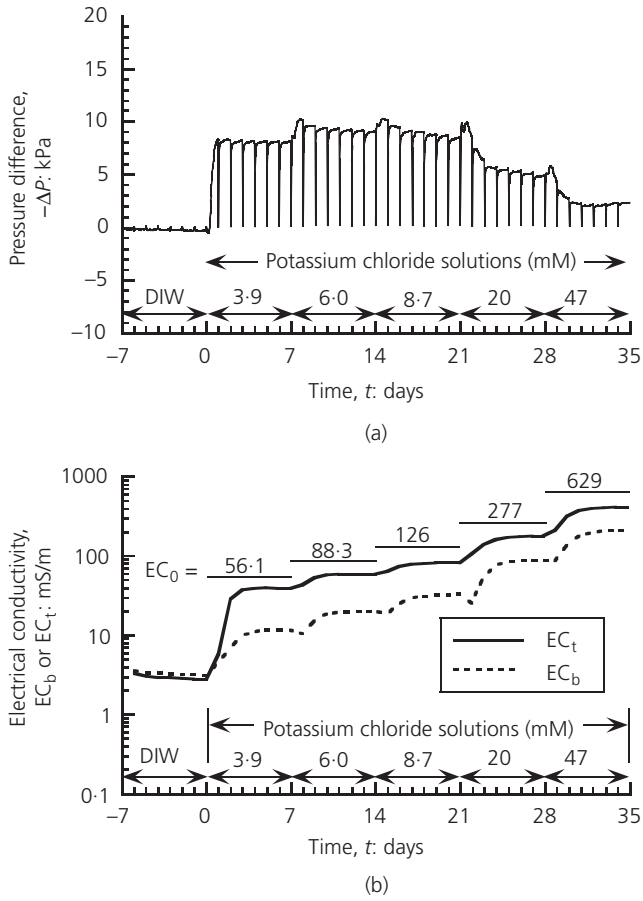

Figure 5. Representative results from a multi-stage membrane test on GCL specimen (σ' = 34·5 kPa): (a) pressure difference, $-\Delta P$, induced across specimen plotted against time; (b) boundary electrical conductivities, EC_b and EC_t, plotted against time (adapted from Kang and Shackelford, 2011)

Once the tests were completed for the 3·9-mM potassium chloride solution, four additional stages were performed in which the source potassium chloride concentration was increased sequentially from 3·9 mM to 6·0, 8·7, 20 and 47 mM. Each stage lasted 7 days, which was sufficient in all cases to achieve steady ΔP, EC_t, and EC_b.

In each stage, the chlorine concentrations in samples of the circulation outflows from the top and bottom specimen boundaries (C_t and C_b, respectively, in Figure 4) were estimated from the relationship between solution EC and potassium chloride concentration in Figure 3. This approach for estimating chlorine concentrations was considered sufficiently accurate for this study, given that the GCL specimens were permeated with DIW to remove most of the excess soluble salts from the pore water of the specimens before testing. As a result of this permeation step, the contribution of soluble salts to EC_t and EC_b was small. Also, although cation exchange of K^+ for Na^+ (the predominant exchangeable cation species in the GCL) likely was occurring during the tests, the EC calibration curves for potassium chloride and sodium chloride in Figure 3 are reasonably similar. Based on these calibration curves, chlorine concentrations estimated from the sodium chloride curve would be about 14% higher than those estimated from the potassium chloride curve.

Determination of D_s^* for each testing stage was based on the steady-state approach in which the estimated chlorine concentrations were converted to cumulative moles per unit area, Q_t, and plotted as a function of elapsed time, t (Shackelford, 1991). Values of D_s^* were then computed using the following expression:

$$D_s^* = -\left(\frac{\Delta Q_t}{\Delta t}\right)\frac{L}{n\Delta C_{ave}} = -\left(\frac{\Delta Q_t}{\Delta t}\right)\frac{L}{n\left(C_{b,ave} - C_{t,ave}\right)} \quad (6)$$

σ': kPa	C_{ot}: mM	L: mm	n: —	Values at steady state								
				EC_t: mS/m	EC_b: mS/m	C_t: mM	C_b: mM	$-\Delta C_{ave}$: mM	$-\Delta P$: kPa	ω: —	$\Delta Q_t/\Delta t$: mmol/m² day	D_s^*: $\times 10^{-10}$ m²/s
34·5	0	9·5	0·81	2·95	3·10	—	—	—	—	—	—	—
	3·9	9·3	0·80	39·2	11·6	2·68	0·63	2·98	8·18	0·561	2·76	1·26
	6·0	9·1	0·80	58·5	20·0	4·12	1·25	4·43	9·01	0·418	5·56	1·66
	8·7	9·0	0·79	81·5	32·7	5·81	2·19	6·16	8·57	0·286	9·87	2·08
	20	8·7	0·79	177	88·3	12·9	6·31	13·3	4·90	0·076	28·1	2·69
	47	8·7	0·79	415	211	30·3	15·2	31·1	2·29	0·015	68·2	2·80
103	0	9·5	0·80	2·08	1·65	—	—	—	—	—	—	—
	3·9	9·4	0·80	46·8	7·17	3·22	0·41	3·35	9·48	0·584	2·13	0·86
	6·0	9·3	0·80	67·6	16·8	4·84	1·12	4·86	11·0	0·461	4·99	1·39
	8·7	9·3	0·80	95·9	27·8	6·91	1·93	6·83	11·0	0·328	8·70	1·71
	20	9·2	0·80	203	72·6	14·7	5·25	14·7	11·0	0·152	23·2	2·12
	47	9·2	0·79	460	185	33·5	13·6	33·5	11·2	0·068	60·2	2·41
172	0	8·2	0·77	2·62	3·14	—	—	—	—	—	—	—
	3·9	8·2	0·77	47·6	9·09	3·25	0·441	3·36	12·1	0·719	1·96	0·72
	6·0	8·1	0·77	67·5	13·8	4·81	0·791	5·01	15·2	0·628	3·50	0·86
	8·7	8·0	0·76	94·9	22·5	6·87	1·43	7·07	16·6	0·484	6·53	1·13
	20	7·9	0·76	202	63·5	14·7	4·47	15·1	16·6	0·226	19·9	1·59
	47	7·9	0·76	452	175	33·2	12·7	33·7	16·1	0·098	57·0	2·02
241	0	6·4	0·70	2·95	3·63	—	—	—	—	—	—	—
	3·9	6·3	0·69	46·3	7·70	3·18	0·301	3·39	12·9	0·784	1·37	0·43
	6·0	6·1	0·68	71·4	13·2	5·05	0·711	5·17	16·0	0·635	3·18	0·64
	8·7	5·8	0·67	101	22·5	7·22	1·40	7·26	16·2	0·459	6·24	0·87
	20	5·7	0·66	212	60·8	15·5	4·23	15·6	17·6	0·230	18·5	1·18
	47	5·6	0·66	464	148	33·7	10·7	35·0	18·2	0·106	48·6	1·38

σ', effective stress; C_{ot}, source potassium chloride concentration; L, specimen thickness; n, total porosity; EC_t and EC_b, EC of outflows from top and bottom boundaries, respectively; C_t and C_b, molar chlorine concentrations in outflows from top and bottom boundaries, respectively; ΔC_{ave}, average boundary concentration difference; ΔP, induced pressure difference; ω, membrane efficiency coefficient computed based on ΔC_{ave} (see Kang and Shackelford, 2011); $\Delta Q_t/\Delta t$, diffusive molar chlorine flux; D_s^*, effective salt-diffusion coefficient.

Table 1. Summary of multi-stage membrane test results for four GCL specimens

where $\Delta Q_t/\Delta t$ is the steady-state diffusive molar flux (i.e., the slope of the Q_t against t data at steady state), L is the specimen thickness, and $C_{b,ave}$ and $C_{t,ave}$ are the average molar Cl^- concentrations at the bottom and top specimen boundaries, as follows:

$$C_{b,ave} = \left(\frac{C_b + C_{ob}}{2}\right);\ C_{t,ave} = \left(\frac{C_t + C_{ot}}{2}\right) \tag{7}$$

Membrane efficiency coefficients at steady state were also computed from average boundary concentrations, as follows:

$$\omega = \frac{-\Delta P}{2RT\Delta C_{ave}} = \frac{-\Delta P}{2RT\left(C_{b,ave} - C_{t,ave}\right)} \tag{8}$$

where R is the universal gas constant (8·314 J/mol K) and T is absolute temperature (K).

Results and discussion

Differential pressures induced across the GCL specimens, $-\Delta P$ (>0), and EC values measured in the outflows from the top and bottom specimen boundaries (EC_t and EC_b, respectively) were plotted as a function of cumulative elapsed time for each test (see Kang and Shackelford, 2011), as illustrated in Figure 5 for the specimen consolidated at $\sigma' = 34{\cdot}5$ kPa. In each test, an initial $-\Delta P$ was induced across the specimen while circulating DIW across both boundaries (see Figure 5a). This initial $-\Delta P$ was nearly zero in all cases and was subtracted from the $-\Delta P$ measured after introducing the potassium chloride solutions when computing ω using Equation 8. Likewise, initial EC_t and EC_b values greater than that of the DIW were measured during DIW circulation across both boundaries, owing to the release of residual salts that were not removed during permeation. These initial EC values remained reasonably steady during DIW circulation (e.g., see Figure 5b) and were subtracted from the EC_t and EC_b values used to estimate the boundary potassium chloride concentrations.

Effective diffusion coefficients

The results of the multi-stage tests are summarized in Table 1. The steady-state diffusive fluxes, $\Delta Q_t/\Delta t$, were obtained from the slopes of the steady (linear) portions of the Q_t against t plots for each stage, which are presented in Figure 6 for the stages conducted with $C_{ot} = 3{\cdot}9$ mM. The resulting values of D_s^* (computed using Equations 6 and 7) are shown in Table 1, along with the steady-state values of ω reported previously by Kang and Shackelford (2011).

The results in Table 1 and Figure 7a show that the values of ω for a given specimen decreased with increasing source potassium chloride concentration, C_{ot}, due to progressively greater collapse of the DDLs surrounding the clay particles as the salt diffused into the GCL pores at progressively higher concentrations (see Kang

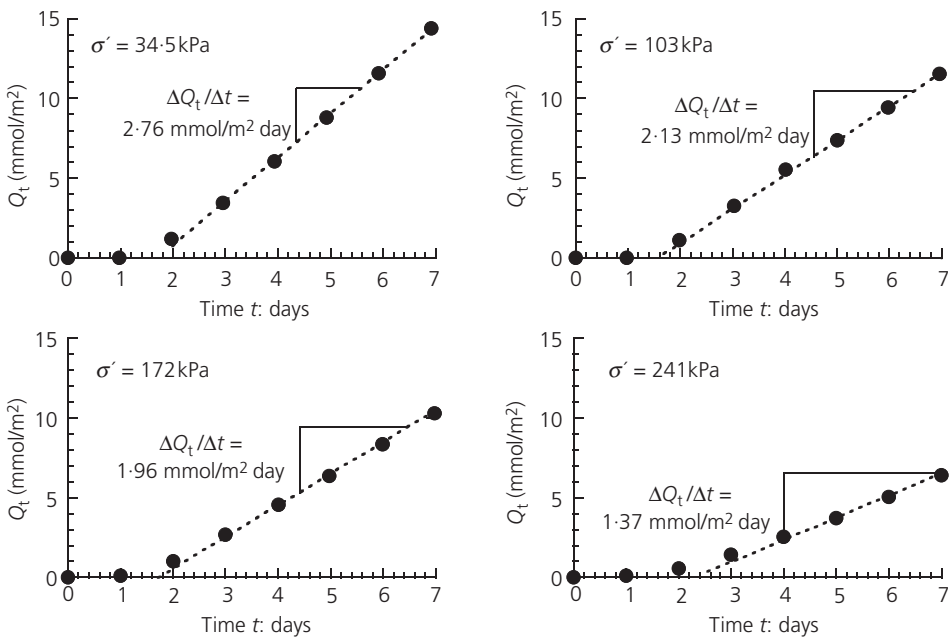

Figure 6. Cumulative moles of chlorine per unit area, Q_t, diffused through four GCL specimens (σ' = 34·5, 103, 172, and 241 kPa, respectively) in the first stage of each multi-stage membrane test (C_{ot} = 3·9 mM potassium chloride)

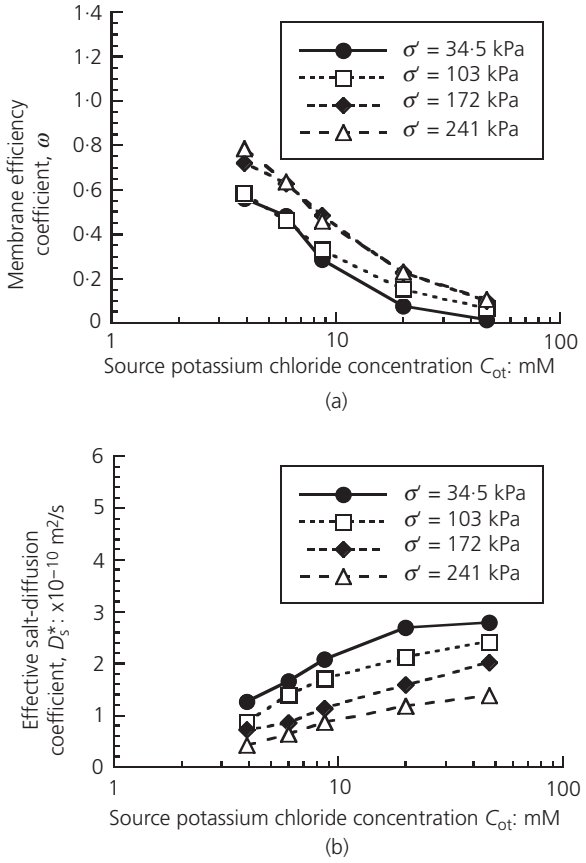

Figure 7. Membrane efficiency coefficients (adapted from Kang and Shackelford, 2011) (a) and effective salt-diffusion coefficients (b) as a function of source potassium chloride concentration for GCL specimens consolidated at different effective stresses (σ' = 34·5, 103, 172, and 241 kPa)

and Shackelford, 2011). The progressively greater collapse of the DDLs with increasing C_{ot} also increased the sizes of the pore spaces available for solute diffusion, resulting in an increase in D_s^* (Malusis and Shackelford, 2002b). This trend of increasing D_s^* with increasing C_{ot} was evident in each of the tests in this study, as illustrated in Figure 7b. Although the lowest C_{ot} tested in this study was 3·9 mM, the trends in Figure 7a and b indicate that progressively lower values of C_{ot} would yield progressively higher ω (toward the theoretical upper bound of $\omega = 1$) and progressively lower D_s^* (toward the theoretical lower bound of $D_s^* = 0$).

The results in Figure 7 also reveal trends of increasing ω and decreasing D_s^* with increasing σ' for a given C_{ot}, indicating an overall reduction in pore size with increasing consolidation. Although a higher σ' did not yield a lower total porosity, n, in all cases, a general trend of decreasing n with increasing σ' is evident in Table 1. As noted by Kang and Shackelford (2011), a decrease in void space would be expected to restrict solute passage and increase membrane efficiency.

The relationships between D_s^* and ω for the specimens in this study are illustrated in Figure 8. Each of the specimens exhibited a decrease in D_s^* with increasing ω, consistent with the prior results illustrated in Figure 2a. Moreover, the decreases in D_s^* are approximately linear, such that the best-fit linear regressions shown in Figure 8 intersect the $D_s^* = 0$ axis within the range $\omega = 1{\cdot}0 \pm 0{\cdot}1$ in all cases. Theoretically, $D_s^* = 0$ should correspond to $\omega = 1$, since an ideal membrane, by definition, completely restricts solute passage. This theoretical consideration is well supported by the data in Figure 8.

The theoretical maximum value of D_s^* for each specimen, corresponding to zero membrane efficiency (i.e., $\omega = 0$), was estimated from the linear regressions in Figure 8. As discussed previously, values of D_s^* at $\omega = 0$ were interpreted as matrix diffusion coefficients, D_{se}. The linear regressions yielded values of D_{se} ranging from $1{\cdot}5 \times 10^{-10}$ to $2{\cdot}9 \times 10^{-10}$ m²/s and decreasing with increasing σ' (see Figure 9). This trend of decreasing D_{se} with increasing σ' was expected, given the aforementioned trends of decreasing D_s^* and increasing ω (for a given C_{ot}) with increasing σ'.

Restrictive tortuosity factors

Values of the restrictive tortuosity factor, τ_r, for the GCL specimens were computed using Equation 3 (i.e., $\tau_r = D_s^*/D_{se}$) for each testing stage based on the D_s^* values in Table 1 and the D_{se} values in Figure 9. These values of τ_r are plotted as a function of ω in Figure 10, along with the best-fit regression of the linear relationship given by Equation 4 (i.e., $\tau_r = 1 - \omega$). The results illustrate that τ_r closely follows the linear trend given by Equation 4 ($R^2 = 0{\cdot}976$), regardless of the σ' employed in the test. Thus, the results in this study provide compelling evidence that Equation 4 may be a valid expression for relating τ_r to ω for clay membranes. However, these results are limited to potassium chloride solutions and GCLs containing 100% conventional sodium bentonite. Similar analyses as described herein must be performed for other chemical solutions and other types of barrier materials exhibiting membrane behaviour before a more robust conclusion can be made regarding the general applicability of Equation 4 for clay membranes.

Conclusions

The results of this study demonstrate that effective salt-diffusion coefficients, D_s^*, for a geosynthetic clay liner (GCL) are dependent on both the source concentration of the salt, C_o, and the effective stress, σ', applied to the GCL. In addition, the concentration dependence of D_s^* was related directly to the concentration dependence of membrane efficiency, which has been reported in several previously published studies on clay membranes. In this study, D_s^* for each GCL specimen approached a maximum value at zero membrane efficiency ($\omega = 0$) and decreased linearly toward $D_s^* = 0$ as the membrane behaviour approached the ideal condition ($\omega = 1$). Thus, the results support the theoretical requirement that $D_s^* = 0$ for an ideal membrane that completely restricts solute passage.

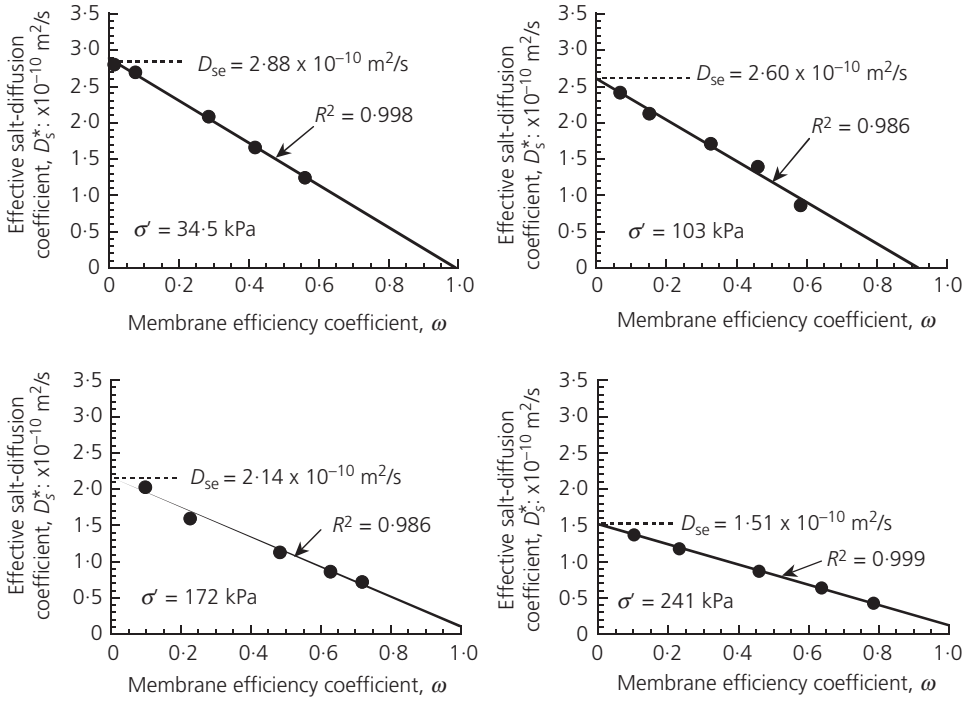

Figure 8. Effective salt-diffusion coefficients, D_s^*, as a function of the membrane efficiency coefficient, ω, for GCL specimens consolidated at different effective stresses (σ' = 34·5, 103, 172, and 241 kPa)

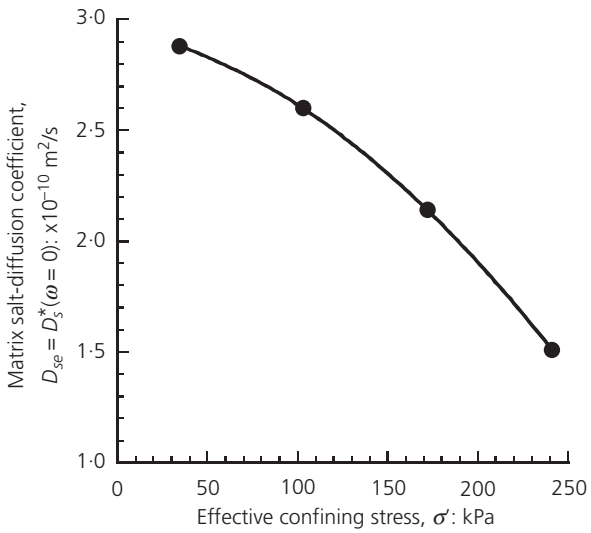

Figure 9. Matrix salt-diffusion coefficients, D_{se}, as a function of effective confining stress, σ'

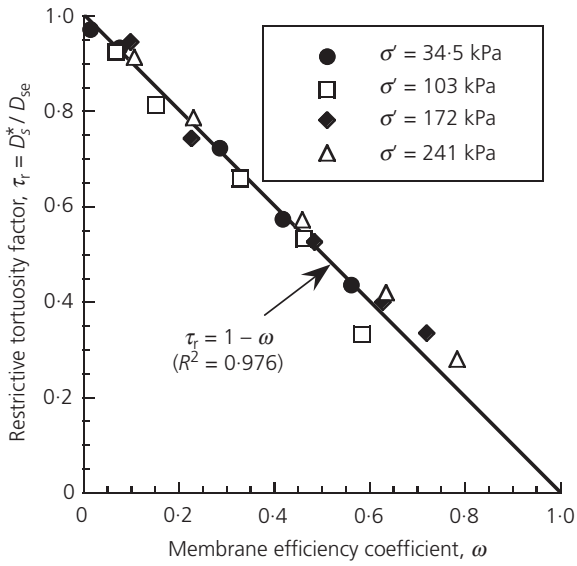

Figure 10. Restrictive tortuosity factors, τ_r, as a function membrane efficiency coefficient, ω, for GCL specimens consolidated at different effective stresses (σ' = 34·5, 103, 172, and 241 kPa)

The maximum values of D_s^* corresponding to $\omega = 0$, designated herein as D_{se}, are considered to be governed solely by the matrix tortuosity or by the tortuosity associated with the geometry of the interconnected pores. The D_{se} values were shown to decrease with increasing σ' due to an overall reduction in pore size with increasing σ'. In contrast, the values of D_s^* corresponding to $\omega > 0$ are considered to be a function of both the matrix tortuosity factor, τ_m, and a restrictive tortuosity factor, τ_r, that accounts for solute exclusion owing to membrane behaviour. Values of τ_r computed for the GCL specimens in this study were shown to decrease linearly with increasing ω, such that the relationship between τ_r and ω is well represented by the expression $\tau_r = 1 - \omega$ that has been proposed previously on the basis of theoretical studies. Thus, the results presented in this study provide compelling evidence in support of the hypothesis that $\tau_r = 1 - \omega$ is a valid expression for clay membrane barriers and can be used in coupled solute transport model formulations to explicitly account for the influence of membrane behaviour on D_s^*. Such an approach would be reasonable, provided that the input value of ω is appropriate for the given chemical solution, source concentration and barrier being modeled. Since this study was limited to potassium chloride solutions and GCLs containing 100% conventional sodium bentonite, additional testing is warranted to assess the applicability of this expression for other chemical solutions and other barrier materials that exhibit membrane behaviour.

Acknowledgements

Financial support for portions of this work was provided by the US National Science Foundation (NSF), Arlington, VA, under Grants CMS-0099430 entitled, “Membrane Behavior of Clay Soil Barrier Materials,” and CMS-0624104 entitled, “Enhanced Clay Membrane Barriers for Sustainable Waste Containment.” The opinions expressed in this paper are solely those of the writers and are not necessarily consistent with the policies or opinions of the NSF.

This paper is a modified version of an earlier paper by the same authors entitled, “Influence of membrane efficiency on solute diffusion through a GCL,” which was published in *Coupled Phenomena in Environmental Geotechnics* (Proceedings of the 2013 International Symposium, ISSMGE TC215, Torino, Italy, July 1–3, 2013). The authors are grateful to the Italian Geotechnical Society (Associazione Geotecnica Italiana, Rome, Italy) and Taylor & Francis Group (London, UK) for granting permission to publish this version in *Environmental Geotechnics*.

REFERENCES

Di Emidio G (2010) *Hydraulic and Chemico-Osmotic Performance of Polymer Treated Clays.* PhD Dissertation, Ghent University, Ghent, Belgium.

Dominijanni A (2005) *Osmotic Properties of Clay Soils*. PhD Dissertation, Politecnico di Torino, Torino, Italy.

Dominijanni A (2013) Osmotic phenomena in bentonites. Coupled phenomena in environmental geotechnics: From theoretical and experimental research to practical applications. In *Proceedings of the International Symposium, ISSMGE TC 215, Torino, Italy* (Manassero M, Dominijanni A, Foti S and Musso G (eds.)). Taylor & Francis, London, UK, pp. 169–180.

Dominijanni A and Manassero M (2012) Modelling the swelling and osmotic properties of clay soils: Part II. The physical approach. *International Journal of Engineering Science* **51**: 51–73.

Dominijanni A, Manassero M and Puma S (2013) Coupled chemical-hydraulic-mechanical behaviour of bentonites. *Géotechnique* **63(3)**: 191–205.

Greenberg J, Mitchell J and Witherspoon P (1973) Coupled salt and water flows in a groundwater basin. *Journal of Geophysical Research* **78(27)**: 6341–6353.

Henning J, Evans J and Shackelford C (2006) Membrane behavior of soil-bentonite slurry trench cutoff wall backfill. *Journal of Geotechnical and Geoenvironmental Engineering ASCE* **132(10)**: 1243–1249.

Kang J (2008) *Membrane Behavior of Clay Liner Materials.* PhD Dissertation, Colorado State University, Fort Collins, CO, USA.

Kang J and Shackelford C (2009) Clay membrane testing using a flexible-wall cell under closed-system boundary conditions. *Applied Clay Science* **136(10)**: 1368–1382.

Kang J and Shackelford C (2010) Membrane behavior of compacted clay liners. *Journal of Geotechnical and Geoenvironmental Engineering ASCE* **44(1–2)**: 43–58.

Kang J and Shackelford C (2011) Consolidation enhanced membrane behavior of a geosynthetic clay liner. *Geotextiles and Geomembranes* **29(6)**: 544–556.

Keijzer T, Kleingeld P and Loch J (1999) Chemical osmosis in compacted clayey material and the prediction of water transport. *Engineering Geology* **53(2)**: 151–159.

Kemper W, Maasland D and Porter L (1964) Mobility of water adjacent to mineral surfaces. *Soil Science Society of America Proceedings* **28(2)**: 164–167.

Kharaka Y and Berry F (1973) Simultaneous flow of water and solutes through geological membranes: I. Experimental investigation. *Geochimica et Cosmochimica Acta* **37(12)**: 2577–2603.

Malusis M and Shackelford C (2002a) Chemico-osmotic efficiency of a geosynthetic clay liner. *Journal of Geotechnical and Geoenvironmental Engineering ASCE* **128(2)**: 97–106.

Malusis M and Shackelford C (2002b) Coupling effects during steady-state solute diffusion through a semipermeable clay membrane. *Environmental Science and Technology* **36(6)**: 1312–1319.

Malusis M and Shackelford C (2004a) Explicit and implicit coupling during solute transport through clay membrane barriers. *Journal of Contaminant Hydrology* **72(1–4)**: 259–285.

Malusis M and Shackelford C (2004b) Predicting solute flux through a clay membrane barrier. *Journal of Geotechnical and Geoenvironmental Engineering ASCE* **130(5)**: 477–487.

Malusis M, Shackelford C and Olsen H (2001) Laboratory apparatus to measure chemico-osmotic efficiency coefficients for clay soils. *Geotechnical Testing Journal ASTM* **24(3)**: 229–242.

Malusis M, Shackelford C and Olsen H (2003) Flow and transport through clay membrane barriers. *Engineering Geology* **70(2–3)**: 235–248.

Malusis M, Shackelford C and Maneval J (2012) Critical review of coupled flux formulations for clay membranes based on nonequilibrium thermodynamics. *Journal of Contaminant Hydrology* **138**–**139**: 40–59.

Manassero M and Dominijanni A (2003) Modelling the osmosis effect on solute migration through porous media. *Géotechnique* **53(5)**: 481–492.

Marine I and Fritz S (1981) Osmotic model to explain anomalous hydraulic heads. *Water Resources Research* **17(1)**: 73–82.

Mazzieri F, Di Emidio G and Van Impe P (2010) Diffusion of calcium chloride in a modified bentonite: Impact of osmotic efficiency and hydraulic conductivity. *Clays and Clay Minerals* **58(3)**: 351–363.

Neuzil C (1986) Groundwater flow in low-permeability environments. *Water Resources Research* **22(8)**: 1163–1195.

Shackelford C (1991) Laboratory diffusion testing for waste disposal — A review. *Journal of Contaminant Hydrology* **7(3)**: 177–217.

Shackelford C (2013) Membrane behavior of bentonite-based barriers: State of the art. Coupled phenomena in environmental geotechnics: From theoretical and experimental research to practical applications. In *Proceedings of the International Symposium, ISSMGE TC 215, Torino, Italy* (Manassero M, Dominijanni A, Foti S and Musso G (eds.)). Taylor & Francis, London, UK, pp. 45–60.

Shackelford C and Daniel D (1991) Diffusion in saturated soil: I. Background. *Journal of Geotechnical Engineering ASCE* **117(3)**: 467–484.

Shackelford C and Moore M (2013) Fickian diffusion of radionuclides for engineered containment barriers: Diffusion coefficients, porosities, and complicating issues. *Engineering Geology* **152(1)**: 133–147.

Yeo S, Shackelford C and Evans J (2005) Membrane behavior of model soil-bentonite backfill mixtures. *Journal of Geotechnical and Geoenvironmental Engineering ASCE* **131(4)**: 418–429.

Young A and Low P (1965) Osmosis in argillaceous rocks. *Bulletin of the American Association of Petroleum Geologists* **49(7)**: 1004–1008.

WHAT DO YOU THINK?

To discuss this paper, please submit up to 500 words to the editor at www.editorialmanager.com/envgeo by 1 January 2014. Your contribution will be forwarded to the author(s) for a reply and, if considered appropriate by the editorial panel, will be published as a discussion in a future issue of the journal.